

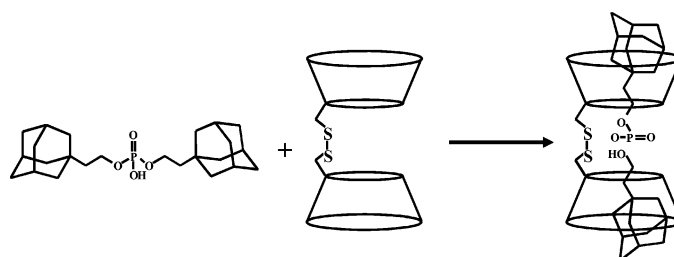
Chelate Effect in Cyclodextrin Dimers: A Computational (MD, MM/PBSA, and MM/GBSA) Study

Ivan Beà,[†] Martin G. Gotsev,[‡] Petko M. Ivanov,^{*,†,‡} Carlos Jaime,^{*,†} and Peter A. Kollman[§]

Departament de Química, Universitat Autònoma de Barcelona, 08193 Bellaterra, Spain, Institute of Organic Chemistry with Centre of Phytochemistry, Bulgarian Academy of Sciences, ul. Acad. G. Bonchev, bloc 9, 1113 Sofia, Bulgaria, and Department of Pharmaceutical Chemistry, University of California, San Francisco, California 94143

carlos.jaime@uab.es; ivanov@bas.bg

Received November 30, 2005



The complexation of an adamantyl-phosphate derivative with one β -cyclodextrin, with two β -cyclodextrins, and with two β -cyclodextrins dimerized with a disulfide bridge was studied by computational methods (MD, MM/PBSA, and MM/GBSA) to analyze and rationalize the chelate effect. Although this effect is usually explained by invoking favorable entropy contribution due to the preorganization of the ligand, it has been determined experimentally that in this case it is enthalpy-driven. The computational results are in accord with this finding, although the entropy contribution due to the solvent structural organization around the complex is crucial for the final estimates of the free energy of complexation.

Introduction

The chelate effect, invoked to justify that bidentate ligands give values of formation constants much larger than those of monodentate ligands, is classically explained by the entropy contribution to the free energy of the process produced by the preceding arrangement of the ligand.¹ The chelate effect is of essential importance in inorganic chemistry² where metallic cations are normally surrounded by various ligands. Nevertheless, recent developments in supramolecular chemistry (more precisely, in host/guest chemistry) revealed the importance of the chelate effect in organic chemistry as well.^{3,4} Among the systems studied are those having cyclodextrin dimers as a host.⁵

The thermodynamics of the complexation of several guests with cyclodextrin dimers (linked with different spacers) were studied experimentally in aqueous solution.⁶ The chelate effect

[†] Universitat Autònoma de Barcelona.

[‡] Bulgarian Academy of Sciences.

[§] University of California, San Francisco.

(1) Orgel, L. E. *An Introduction to Transition-Metal Chemistry: Ligand-Field Theory*; John Wiley & Sons: New York, 1960; p 15.

(2) (a) Siemeling, U.; Türk, T.; Schoeller, W. W.; Redshaw, C.; Gibson, V. C. *Inorg. Chem.* **1998**, *37*, 4738–4739. (b) Sjövall, S.; Andersson, C.; Wendt, O. F. *Organometallics* **2001**, *20*, 4919–4926. (c) Emmenegger, F.; Schlaepfer, C. W.; Stoeckli-Evans, H.; Piccand, M.; Piekarski, H. *Inorg. Chem.* **2001**, *40*, 3884–3888. (d) Bernard, C.; Christian, B.; Georges, W. *Phys. Chem. Chem. Phys.* **2002**, *4*, 5716–5729. (e) Christian, B.; Bernard, C.; Georges, W. *J. Phys. Chem. A* **2002**, *106*, 6487–6498. (f) Hossain, M. A.; Kang, S. O.; Powell, D.; Bowman-James, K. *Inorg. Chem.* **2003**, *42*, 1397–1399.

(3) Breslow, R.; Belvedere, S.; Gershell, L.; Leung, D. *Pure Appl. Chem.* **2000**, *72*, 333–342.

(4) Steed, J. W.; Atwood, J. L. *Supramolecular Chemistry*; John Wiley & Sons, Ltd.: Chichester, U.K., 2000.

(5) (a) Haskard, C. A.; Easton, C. J.; May, B. L.; Lincoln, S. F. *J. Phys. Chem.* **1996**, *100*, 14457–14461. (b) Moser, J. G.; Ruebner, A.; Vervoorts, A.; Wagner, B. *J. Incl. Phenom. Mol. Recogn. Chem.* **1996**, *25*, 29–34. (c) Ikeda, H.; Nishikawa, S.; Takaoka, J.; Akiike, T.; Yamamoto, Y.; Ueno, A.; Toda, F. *J. Inclusion Phenom. Mol. Recognit. Chem.* **1996**, *25*, 133–136. (d) Shi, X. Y.; Zhang, Y. Q.; Han, J. H.; Fu, R. N. *Chromatographia* **2000**, *52*, 200–204. (e) Van Bommel, K. J. C.; De Jong, M. R.; Metselaar, G. A.; Verboom, W.; Huskens, J.; Hulst, R.; Kooijman, H.; Spek, A. L.; Reinhoudt, D. N. *Chem.–Eur. J.* **2001**, *7*, 3603–3615. (f) Narita, M.; Itoh, J.; Kikuchi, T.; Hamada, F. *J. Inclusion Phenom. Macrocyclic Chem.* **2002**, *42*, 107–114. (g) De Jong, M. R.; Berthault, P.; Van Hoek, A.; Visser, A. J. W. G.; Huskens, J.; Reinhoudt, D. N. *Supramol. Chem.* **2002**, *14*, 143–151. (h) Liu, Y.; Li, L.; Zhang, H. Y.; Song, Y. *J. Org. Chem.* **2003**, *68*, 527–236. (i) Ikeda, H.; Matsuhita, A.; Ueno, A. *Chem.–Eur. J.* **2003**, *9*, 4907–4910. (j) Mulder, A.; Jukovic, A.; Huskens, J.; Reinhoudt, D. N. *Org. Biomol. Chem.* **2004**, *3*, 1748–1755. (k) Liu, Y.; Song, Y.; Chen, Y.; Li, X. Q.; Ding, F.; Zhong, R. Q. *Chem.–Eur. J.* **2004**, *10*, 3685–3696. (m) Liu, Y.; Zhao, Y. L.; Chen, Y.; Ding, F.; Chen, G. S. *Bioconjugate Chem.* **2004**, *15*, 1236–1245. (l) Liu, Y.; Li, L.; Chen, Y.; Yu, L.; Fan, Z.; Ding, F. *J. Phys. Chem. B* **2005**, *109*, 4129–4134. (n) Nascimento, C. S., Jr.; Anconi, C. P. A.; Dos Santos, H. F.; De Almeida, W. B. *J. Phys. Chem. A* **2005**, *109*, 3209–3219. (o) Mulder, A.; Huskens, J.; Reinhoudt, D. N. *Eur. J. Org. Chem.* **2005**, 838–846.

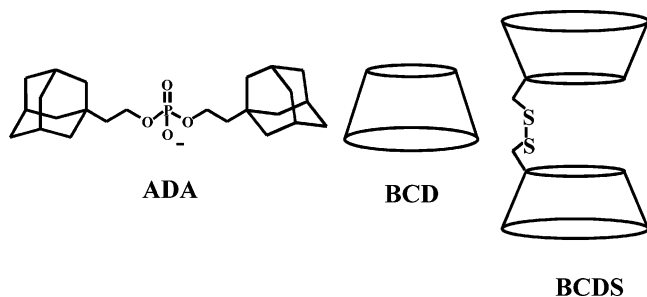


FIGURE 1. Structures of the di-2-(1-adamantyl)ethyl hydrogenophosphate molecule in anionic (**ADA**) form, β -cyclodextrin (**BCD**), and S–S linked β -cyclodextrin dimer (**BCDS**).

TABLE 1. Experimental⁶ Formation Constants, K_f (M^{-1}), and Thermodynamic Data (kcal/mol) for the Complexation of **ADA** with **BCDS** (**ADA/BCDS**), with One **BCD** (**ADA/BCD**), with the Second **BCD** (**ADA/(BCD+BCD)**), and for the Total Complexation with Two **BCDs** (**ADA/2BCD**)

complex	K_f	ΔG	ΔH	$T\Delta S$
ADA/BCDS	1.8×10^7	-9.89	-16.15	-6.26
ADA/BCD	2.3×10^5	-7.30	-7.00	0.30
ADA/(BCD+BCD)	4.4×10^3	-4.97	-3.84	1.13
ADA/2BCD		-12.27	-10.84	1.43

(the strong binding of ditopic substrates) was assigned to be entirely due to an improved enthalpy of binding in these cases. Moreover, the entropy of ditopic binding was determined less favorable than for the monodentate binding.^{3,6} The complexation of di-2-(1-adamantyl)ethyl hydrogenophosphate (**ADA**) at pH = 7.0, with either β -cyclodextrin, **BCD**, or a β -cyclodextrin dimer linked by an S–S bridge, **BCDS** (Figure 1), was among the cases considered. The results of the experimental study, Table 1, show that the formation constant for the first cyclodextrin (**ADA/BCD**) is 50 times bigger than that for the second cyclodextrin (**ADA/(BCD + BCD)**). It was proposed⁶ that the first cyclodextrin interferes geometrically with the binding of the second cyclodextrin. The enthalpy of binding for **ADA/BCDS** is ca. 5 kcal/mol more favorable than for the binding of **ADA** with two **BCD** (**ADA/2BCD**). However, the free energy for the complexation with the two independent **BCD** units is higher than for the complexation with the **BCDS**. This originates from the decrease of the entropy for the chelate binding, in contradiction with the classical perception of the chelate effect. The effect of the solvent has been invoked in order to explain the observation (enthalpy/entropy compensation): improved solvation lowers enthalpy and lessens ΔG at the expense of entropy (diminished solvation provides entropy advantages).

Computational studies aimed at the modeling of such complexations are scarce,⁷ and the reason seems to be the inherent difficulty for computing entropy. Moreover, the solvent that should favor the fragments to approach each other also introduces complexity to the system. Solvation effects can be nowadays reasonably well studied by computational methods,⁸ thus allowing the elucidation of the factors responsible for the unexpected observation.⁶ Another aspect of the usefulness of

performing modeling studies on the chelate binding of a doubly bound guest to a relatively rigidly linked cyclodextrin dimer is the potential ability of the linker to act on the guest when a catalytic group is present in the bridge fragment;³ catalysts were reported for ester hydrolysis based on cyclodextrin dimers.^{9,10} The well-defined geometries of these systems provide appropriate conditions to direct chemical reactions to particular parts of the substrate. The understanding of the chelate effect is of practical significance also for designing effective medicinal compounds. Not only cyclodextrin dimers but also cyclodextrin trimers and tetramers are expected to appear suitable for the purpose.^{3,11} A promising approach has been devised by using a cyclodextrin dimer to assist cancer treatment by photodynamic therapy.¹² Thus using computational methods to elucidate the structure and the energetics of these interesting systems can assist in devising useful applications.

We present in this report the results from molecular dynamics simulations on the complexation process of **ADA** with one and two **BCD** and with the **BCDS** dimer in the presence of explicit water as solvent. Relative binding free energies ΔG , different contributions to ΔG , and the effect of the solvent on the energetics of the process were obtained from MM/PBSA^{13a} and MM/GBSA^{13b} analyses of the MD trajectories. The results helped to understand the complexation process and to evaluate the relative importance of the enthalpy and the entropy in this particular case.

Computational Methodology

The AMBER program¹⁴ and the parm94¹⁵ and parm99^{15b} force fields were used throughout all of this work. Atomic charges for the guest molecule (**ADA**) were obtained by the RESP methodology.^{16,17} The anionic form (deprotonated) was only considered, as the phosphate is supposed to prefer the anionic form in water. The charges for **BCD** and for **BCDS** were taken from a previous study.¹⁸

(8) (a) Leach, A. R. *Molecular Modeling. Principles and Applications*; Longman: Harlow, U.K., 1996; Chapter 9. (b) Chuev, G. N.; Basilevsky, M. V. *Russ. Chem. Rev.* **2003**, *72*, 735–758. (c) Tomasi, J. *Theor. Chem. Acc.* **2004**, *112*, 184–203.

(9) Zhang, B.; Breslow, R. *J. Am. Chem. Soc.* **1997**, *119*, 1676–1681.

(10) Jan, J.; Breslow, R. *Tetrahedron Lett.* **2000**, *41*, 2059–2062.

(11) Finnin, M. S.; Donigian, J. R.; Cohen, A.; Richon, V. M.; Rifkind, R. A.; Marks, P. A.; Breslow, R.; Pavletich, N. A. *Nature* **1999**, *401*, 188–193.

(12) Ruebner, A.; Yang, Z.; Leung, D.; Breslow, R. *Proc. Natl. Acad. Sci. U.S.A.* **1999**, *96*, 14692–14693.

(13) (a) Srinivasan, J.; Cheathan, T. E.; Cieplack, P.; Kollman, P. A.; Case, D. A. *J. Am. Chem. Soc.* **1998**, *120*, 9401–9409. (b) Tsui, V.; Case, D. A. *Biopolymers* **2001**, *56*, 275–291.

(14) (a) Case, D. A.; Pearlman, D. A.; Caldwell, J. W.; Cheathan III, T. E.; Ross, W. S.; Simmerling, C. L.; Darden, T. A.; Merz, K. M.; Stanton, R. V.; Cheng, A. L.; Vincent, J. J.; Crowley, M.; Ferguson, D. M.; Radmer, R. J.; Seibel, G. L.; Singh, U. C.; Weiner, P. K.; Kollman, P. A. *AMBER 5*; University of California: San Francisco, 1997. (b) Case, D. A.; Pearlman, D. A.; Caldwell, J. W.; Cheathan, T. E., III; Wang, J.; Ross, W. S.; Simmerling, C. L.; Darden, T. A.; Merz, K. M.; Stanton, R. V.; Cheng, A. L.; Vincent, J. J.; Crowley, M.; Tsui, V.; Gohlke, H.; Radmer, R. J.; Duan, Y.; Pitera, J.; Massova, I.; Seibel, G. L.; Singh, U. C.; Weiner, P. K.; Kollman, P. A. *AMBER 7*; University of California: San Francisco, 2002.

(15) (a) Cornell, W. D.; Cieplack, P.; Bayly, C. I.; Gould, I. R.; Merz, K. M., Jr.; Ferguson, D. M.; Spellmeyer, D. C.; Fox, T.; Caldwell, J. W.; Kollman, P. A. *J. Am. Chem. Soc.* **1995**, *117*, 5179–5197. (b) Wang, J.; Cieplack, P.; Kollman, P. A. *J. Comput. Chem.* **2000**, *21*, 1049–1074.

(16) Bayly, C. I.; Cieplack, P.; Cornell, W. D.; Kollman, P. A. *J. Phys. Chem.* **1993**, *97*, 10269–10280.

(17) Cornell, W. D.; Cieplack, P.; Bayly, C. I.; Kollman, P. A. *J. Am. Chem. Soc.* **1993**, *115*, 9620–9631.

(18) (a) Beà, I.; Cervelló, E.; Kollman, P. A.; Jaime, C. *Comb. Chem. High Throughput Screening* **2001**, *4* (8), 605–611. (b) Beà, I.; Jaime, C.; Kollman, P. A. *Theor. Chem. Acc.* **2002**, *108*, 286–292.

(6) Zhang, B.; Breslow, R. *J. Am. Chem. Soc.* **1993**, *115*, 9353–9354.

(7) (a) Maletic, M.; Wennemers, H.; McDonald, D. Q.; Breslow, R.; Still, W. C. *Angew. Chem., Int. Ed. Engl.* **1996**, *35*, 1490–1492. (b) Breslow, R.; Yang, Z.; Ching, R.; Trojandt, G.; Odobel, F. *J. Am. Chem. Soc.* **1998**, *120*, 3536–3537. (c) Bicchi, C.; Brunelli, C.; Cravotto, G.; Rubiolo, P.; Galli, M.; Mendicuti, F. *J. Sep. Sci.* **2003**, *26*, 1479–1490. (d) Dobado, J. A.; Benkadour, N.; Melchor, S.; Portal, D. *J. Mol. Struct. (THEOCHEM)* **2004**, *672*, 127–132.

Some additional molecular mechanics force field parameters were derived from ab initio MO calculations or by a comparison with similar parameters in the parm94 force field (O2-P, $K_r = 525.0$, $r_{eq} = 1.566$; OS-P, $K_r = 230.0$, $r_{eq} = 1.670$; OH-P, $K_r = 230.0$, $r_{eq} = 1.670$; OS-CT-OS, $K_\theta = 80.0$, $\theta_{eq} = 126.0$; HC-CT-OS, $K_\theta = 50.0$, $\theta_{eq} = 109.5$; OS-CT-HC, $K_\theta = 50.0$, $\theta_{eq} = 109.5$; units are Å (r_{eq}), kcal/(mol Å²) (K_r), degrees (θ_{eq}), and kcal/(mol radian²) (K_θ). All molecules were solvated by a cubic box of TIP3P waters.¹⁹ Different simulation protocols were executed with the two force fields used.

In the 500 ps simulations with parm94, periodic boundary conditions, 8.0 Å primary cutoff, and 13.0 Å for a secondary cutoff for nonbonded interactions were applied.²⁰ Starting from energy minimized structures, the systems were heated to 300 K in three intervals of 50 ps, followed by 50 ps simulations for achieving equilibration. Production runs of 500 ps were executed with structures sampled every 1.0 ps. A time step of 2.0 fs was used in the simulation at constant temperature and pressure, employing separate temperature scaling factors for the solute atoms and for the solvent, as well as molecule scaling for pressure.

The AMBER program (version 7)^{14b} was used for the 5.0 ns simulations with the most recent parametrization of the AMBER-related additive force fields, parm99.^{15b} The molecular dynamics simulations were run for water solution (a box with TIP3P¹⁹ water molecules) using the particle mesh Ewald (PME) method²¹ for the treatment of the long-range electrostatics. A 9.0 Å distance cutoff was used for direct space nonbonded calculations and a 0.00001 Ewald convergence tolerance for the inclusion of long-range electrostatic contributions. The SHAKE option (tolerance 0.00005 Å) was activated for constraining bonds involving hydrogen atoms. The “solvateBox” command of LEaP was utilized to create a cubic solvent box around the solutes with buffer distances of 10.0 Å between the walls of the box and the closest atoms of the solute. The dimensions of the periodic TIP3P water boxes and the number of water molecules were as follows: **ADN/BCDS** (36.9 Å; 1541); **ADN/2BCD** (head) (40.1 Å; 2023); **ADN/2BCD** (tail) (39.2 Å; 1892); **ADN/2BCD** (crossed) (37.5 Å; 1637); **ADN/BCD** (down) (39.8 Å; 2018); **ADN/BCD** (central) (36.5 Å; 1497); **ADN/BCD** (up) (39.1 Å; 1926); **ADN** (37.2 Å; 1675); **BCDS** (36.4 Å; 1496); **BCD** (36.1 Å; 1529).

We followed practically the same protocol for equilibration tested recently in simulations on large-ring cyclodextrins.²² The preparation of solvated molecules for the simulations comprised several stages: (i) 50000 steps steepest descent minimization with holding the solute fixed with positional restraints; (ii) 25.0 ps unrestrained MD were run at 100 K on the water alone while holding the solutes constrained (this is the stage of the equilibration process where the bulk of the water relaxation takes place); (iii) gradual release of the restraints on the solutes in a series of minimizations and MD steps: 1000 steps minimization and 3.0 ps MD with 25.0 kcal mol⁻¹ Å position restraints, followed by five rounds of 600 steps minimization, reducing the positional restraints by 5.0 kcal mol⁻¹ Å each run; (iv) 50.0 ps MD simulation after heating the system from 100 to 300 K using the default value for the time constant for heat bath coupling; (v) the equilibration process was completed with an additional 500 ps simulation at 300 K. The productive runs

(19) Jorgensen, W. L.; Chandrasekhar, J.; Madura, J. D.; Impey, R. W.; Klein, M. L. *J. Chem. Phys.* **1983**, *79*, 926–935.

(20) All nonbonded interactions were calculated between atoms separated by less than 8 Å (short-range); interactions between atoms separated by 8–13 Å (long-range) were calculated only once each 100 steps.

(21) (a) Darden, T.; York, D.; Pedersen, L. *J. Chem. Phys.* **1993**, *98*, 10089–10092. (b) Essmann, U.; Perera, L.; Berkowitz, M. L.; Darden, T.; Lee, H.; Pedersen, L. G. *J. Chem. Phys.* **1995**, *103*, 8577–8593. (c) Sagui, C.; Darden, T. A. In *Simulation and Theory of Electrostatic Interactions in Solution*; Pratt, L. R., Hummer, G., Eds.; American Institute of Physics: Melville, NY, 1999; pp 104–113. (d) Toukmaji, A.; Sagui, C.; Board, J.; Darden, T. *J. Chem. Phys.* **2000**, *113*, 10913–10927.

(22) Ivanov, P. M.; Jaime, C. *J. Phys. Chem. B* **2004**, *108*, 6261–6274.

were performed with a 1.0 fs time step, at 300 K and a constant pressure of 1.0 bar with isotropic position scaling. The simulation time was 5.0 ns. Samplings were taken every 1.0 ps. The computations were performed using the Compaq AlphaSever HPC of the LSF cluster of CIESCA and on a dual Xeon 3.06 GHz platform at IOC-BAS.

The energy for each complex was computed also by the MM/PBSA (Poisson–Boltzmann/Surface Area^{23a}) and the MM/GBSA (Generalized Born^{15b}/Surface Area (LCPO)²⁴) methodology implemented in AMBER; 500 structures from the whole MD trajectories were utilized to estimate the MM/GBSA energies in each case.

The relative free energies of binding were computed as follows:¹³

$$\Delta G_{\text{binding}} = \Delta G_{\text{water}}(\text{complex}) - [\Delta G_{\text{water}}(\text{guest}) + \Delta G_{\text{water}}(\text{host})] \quad (1)$$

The free energies for each species [the complexes, the guest (bisadamantyl-phosphate in its anionic form), and the host (one or two β -cyclodextrins and the S–S linked dimer)], ΔG_{water} , were evaluated by the following scheme:

$$\Delta G_{\text{water}} = E_{\text{gas}} + G_{\text{solvation}} - T\Delta S \quad (2)$$

$$G_{\text{solvation}} = G_{\text{PB(GB)}} + G_{\text{nonpolar}} \quad (3)$$

$$E_{\text{gas}} = E_{\text{internal}}(\text{bond, angle, torsion}) + E_{\text{electrostatic}} + E_{\text{vdW}} \quad (4)$$

where E_{gas} is the total energy in the gas phase, $G_{\text{PB(GB)}} + G_{\text{nonpolar}}$ – solvation free energies of the complexes.

An estimation of the entropy term (ΔS) was obtained using the NMODE module of AMBER.¹⁴ Sampled structures were extracted from the MD trajectory files (6 structures from each 500 ps simulation and 51 structures from each 5.0 ns simulation; the water molecules were removed). The structures were energy-minimized prior to the normal-mode analysis using distance-dependent dielectric constant of $4r_{ij}$ (where r_{ij} is the distance between atom i and atom j). The final entropy estimates for each system (the complex and the individual molecules) were obtained after averaging the computed values for all snapshots.

Results

All complexes and orientations were studied with the anionic form of the phosphate molecule as a guest (designated as **ADA**). Most probably, only the anionic form should exist in aqueous solution owing to the acidity of the phosphate. Counterions were not used in the MD simulations of the anionic complexes, because the proton will preferentially exchange rapidly with water rather than remain near the complex.

MD on Guest and Hosts. The MD simulations for the solvated guest, **ADA**, produced structures that are folded or extended at different stages of the simulation, with the V-shape (folded) however more frequently appearing (Figure 2). The distance between the adamantyl groups (measured between the carbon atoms linked to the spacer) vary from 6.8 Å (folded) to 9.1 Å (extended). Whereas **BCD** does not deform strongly in solution, **BCDS** is quite tensioned. The S–S linkage forces the two **BCD** units to approach each other (Figure 3, 2.0 ns, 4.0 ns). Extended conformations of **BCDS** are also present (Figure 3, 1.0 ns, 5.0 ns). Both structures have very similar total energies (1587.0 (2.0 ns) and 1587.3 (4.0 ns) kcal/mol vs 1586.8 (1.0

(23) (a) Srinivasan, J.; Cheatham, T. E.; Cieplack, P.; Kollman, P. A.; Case, D. A. *J. Am. Chem. Soc.* **1998**, *120*, 9401–9409. (b) Tsui, V.; Case, D. A. *Biopolymers* **2001**, *56*, 275–291.

(24) Weiser, J.; Shenkin, P. S.; Still, W. C. *J. Comput. Chem.* **1999**, *20*, 217–230.

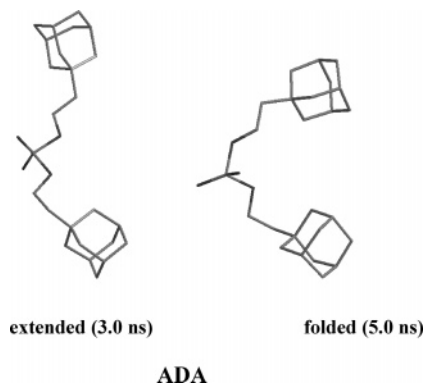


FIGURE 2. Representative conformations of the solvated ADA as obtained from the MD simulations. Hydrogen atoms have been removed for clarity.

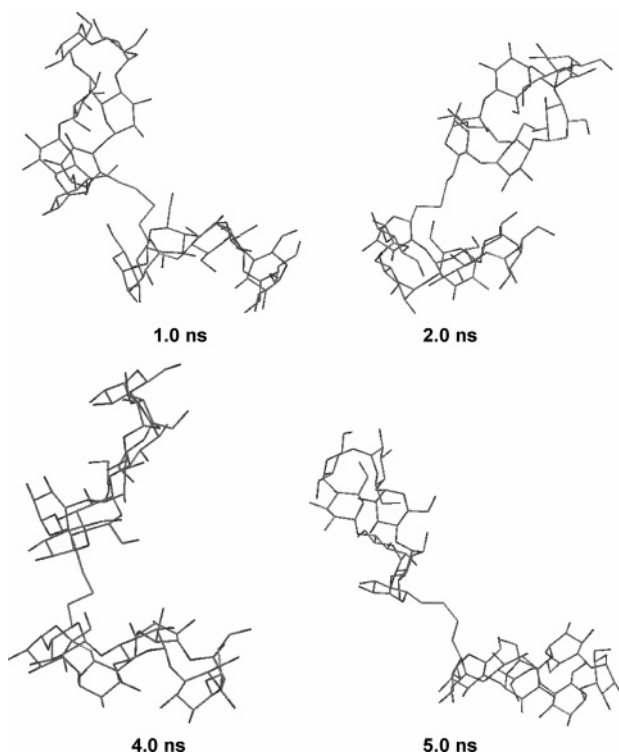


FIGURE 3. Representative structures obtained in the 5.0 ns MD simulations of solvated BCDS. Hydrogen atoms have been removed for clarity.

ns) and 1587.0 (5.0 ns) kcal/mol). The extended conformation presents a better solvation (due to more accessible hydroxyl groups) and a lower internal energy (less tensioned). The preorganized structures (Figure 3, 2.0 ns, 4.0 ns) appear more frequently during the simulation and they can easily develop into a capsule after the substrate enters into the cavity of one of the macro-rings. The S–S linkage provides enough freedom to the two lids to rotate appropriately in order to adjust the substrate. The simulations suggest also a two-stage mechanism for the complex formation, namely, entry of the substrate in the cavity of one of the CDs and subsequent rotation and closure of one of the lids (in addition to the complex formation by the substrate entering simultaneously into the cavities of the two CDs from the side of one of them).

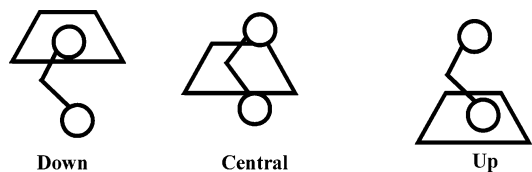


FIGURE 4. Schematic representation of the three initial orientations (down, **D**; central, **C**; and up, **U**) considered for the ADA/BCD complex.

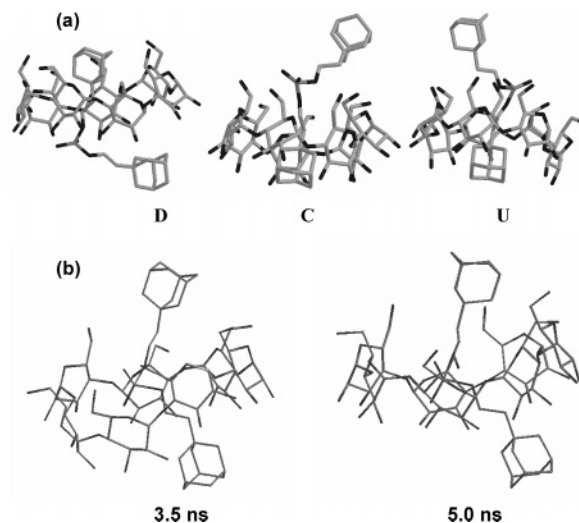


FIGURE 5. (a) Representative conformations obtained in the 500 ps MD simulations of the solvated ADA/BCD in the down (**D**), central (**C**), and up (**U**) orientations, respectively. (b) Snapshots from the 5.0 ns simulation with the central orientation.

MD Simulations of 1:1 Complexes.²⁵ The complexation of the guest with one BCD was studied considering three initial guest orientations, “down” (**D**), “central” (**C**), and “up” (**U**) (Figure 4).

The 500 ps MD simulations with these three orientations afforded preferentially structures presented in Figure 5a. The guest is folded when the **D** and the **C** orientations are used, but not so for **U** (Figure 5a). One adamantyl group in the latter case is included in the cyclodextrin cavity, while the phosphate oxygens interact with the primary hydroxyl rim. The other adamantyl group remains outside the cyclodextrin. The energy analysis indicates that the complex is stabilized by electrostatic and by van der Waals interactions, with the latter interactions more heavily weighted. The prevalence of the complex stabilization by the van der Waals interactions remains even for a value $\epsilon = 1.0$ of the dielectric parameter (Table 2).

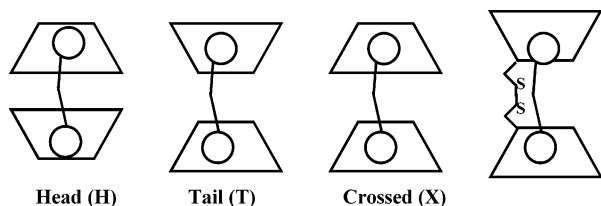
The preferred orientation in the 500 ps simulations is **C** (ADA/BCD-**C**), whereas lower energies were obtained with the parm99 force field and longer simulations (5.0 ns) when starting the simulations from the other two orientations. The results are strongly dependent on the value used for the dielectric parameter. Larger values, e.g., $\epsilon = 4.0$, produce higher stabilization again for the **C** orientation in the 5.0 ns simulations. The overall initial geometry (down, central, and up) can also serve as a designation of the shape of the structures of the complexes

(25) The complexes were designated by using the guest and host names separated by a slash. ADA/BCD means the complex formed between the anionic form of the phosphate and one β -cyclodextrin, whereas ADA/2BCD is the complex with two β -cyclodextrin units and ADA/BCDS is the complex between the anionic form and the S–S linked dimer.

TABLE 2. Energies of Complexation (kcal/mol) of ADA with BCD

	MM/PBSA; parm94 ^a ; 500 ps ^b			MM/GBSA; parm99 ^a ; 5.0 ns ^b					
	down	central	up	down		central		up	
	$\epsilon = 1.0$	$\epsilon = 1.0$	$\epsilon = 1.0$	$\epsilon = 1.0$	$\epsilon = 4.0$	$\epsilon = 1.0$	$\epsilon = 4.0$	$\epsilon = 1.0$	$\epsilon = 4.0$
E_{elec}	-25.7	-6.4	-11.2	-25.5	-6.4	-23.9	-6.0	-11.4	-2.8
E_{vdW}	-33.6	-33.7	-32.0	-36.2	-36.2	-37.7	-37.7	-34.6	-34.6
$E_{\text{gas}} = E_{\text{elec}} + E_{\text{vdW}}$	-59.3	-40.1	-43.2	-61.8	-42.6	-61.7	-43.8	-46.1	-37.5
E_{nonpolar}	-4.4	-4.1	-4.1	-2.7	-2.7	-2.8	-2.8	-2.6	-2.6
$E_{\text{PB/GB}}$	43.9	23.8	28.6	35.4	8.7	38.2	9.4	19.9	4.9
$E_{\text{solvation}}$	39.5	19.7	24.5	32.7	6.0	35.4	6.7	17.3	2.4
$E_{\text{PB/GB+elect}}$	18.2	17.4	17.4	9.9	2.4	14.3	3.5	8.5	2.1
$E_{\text{total,PB/GB}}$	-19.8	-20.4	-18.7	-29.1	-36.6	-26.3	-37.1	-28.8	-35.2

^a Force field. ^b Simulation time.

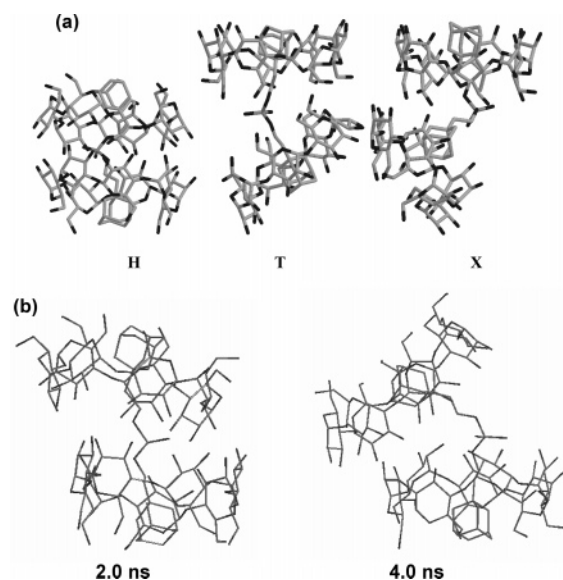
**FIGURE 6.** Schematic representation of the three initial orientations (head, **H**; tail, **T**; and crossed, **X**) considered for the **ADA/2BCD** complexes, and the orientation for the complex with **BCDS**.

during the individual three 5.0 ns simulations (Figures 1S, 2S, and 3S in Supporting Information). The overall appearance of the structures from the three 5.0 ns simulations manifest some specificities: one of the adamantyl groups is inside the cavity, while the other end of the substrate is bent over the macroring (down orientation); the macroring is significantly more distorted in the central orientation than in the other two orientations; one of the adamantyl groups in the up orientation is inside the cavity and the other adamantyl group is above the smaller rim of the macroring but more distant from an average plane of the torus than in the down case (completely extended conformation of the substrate (Figure 3S, 5.0 ns)). An average value of the total energies for the three orientations in Table 2, which are in a dynamical equilibrium in water solution, can be considered as an estimate for the energy of complex formation of **ADA/BCD** (about 27 or 36 kcal/mol for $\epsilon = 1.0$ or 4.0, respectively).

MD Simulations on 2:1 and S–S Dimer Complexes. The complexation of the guest with two cyclodextrins was also studied with 500 ps simulations for three orientations of the two host units: head (**H**), tail (**T**), and crossed (**X**) (Figure 6). Representative structures from the 500 ps MD simulations are presented in Figure 7a.

All structures have the phosphate molecule unfolded and interlinking the two host units of the complex. The complexes with the three orientations were further subjected to the longer 5.0 ns simulation. The van der Waals interactions again present the decisive factor for the complex formation (Table 3). The shape of the suprastructure **ADA/2BCD** vary significantly during the long 5.0 ns simulation: from the normal “cylindrical” form of the cavity enclosed by the two macrorings to significantly displaced and tilted with respect to each other CDs (Figure 7b). Figures 3S, 5S, and 6S in Supporting Information displays snapshots from different stages of the 5.0 ns simulations with the three orientations.

Only one orientation was studied for the complexation of the disulfide-bridged cyclodextrin dimer (Figure 6). Representative structures are displayed in Figure 8. In disagreement with the

**FIGURE 7.** (a) Representative conformations in the 500 ps simulations for the solvated **ADA/2BCD** complexes in the **H**, **T**, and **X** orientations, respectively. (b) Snapshots from the 5.0 ns simulation with the head orientation.

experimentally determined enthalpy estimate,⁶ the binding energy with **BCDS** is smaller than that for the case with two cyclodextrins when only 500 ps simulation is executed. However, the average estimates for **ADA/2BCD** (Table 3; -50.7 and -59.8 kcal/mol for $\epsilon = 1.0$ and 4.0, respectively) from the longer 5.0 ns simulation match the experimental observations: the **ADA/BCDS** complex is characterized with the larger binding energy. This is valid also for a comparison with the binding energies of the **ADA/2BCD** complex in the tail orientation (the two CDs in **BCDS** are in tail orientation to each other). The distance between the two adamantyl groups of the substrate increases to 9.5 Å when it is complexed with the **BCDS**. Figure 7S in Supporting Information displays snapshots from different stages of the 5.0 ns simulation of the **ADA/BCDS** complex.

The comparison of the energy data for **ADA/BCDS** and **ADA/2BCD-T** (5.0 ns simulation) indicates that all energy contributions are similar for the two suprastructures. The S–S linkage forces the two **BCD** units to be positioned closer to each other and to deform. The complexation of **BCDS** with the guest does not alter significantly this molecular geometry.

The binding energy for the complexation of the second **BCD** unit can be also deduced from the binding energies for the 1:1 (Table 2, **C** (central)) and 2:1 (Table 3) complexes. Values of

TABLE 3. Computed Results (kcal/mol) for Energies of Complexation of ADA/2BCD and ADA/BCDS

	ADA/2BCD						ADA/BCDS				
	MM/PBSA AMBER (parm94) ^a 500 ps ^b		MM/GBSA AMBER (parm99) ^a 5.0 ns ^b				MM/PBSA AMBER (parm94) ^a 500 ps ^b		MM/GBSA AMBER (parm99) ^a 5.0 ns ^b		
	H ^c		H ^c		T ^c		X ^c				
	$\epsilon = 1.0$	$\epsilon = 1.0$	$\epsilon = 1.0$	$\epsilon = 4.0$	$\epsilon = 1.0$	$\epsilon = 4.0$	$\epsilon = 1.0$	$\epsilon = 4.0$	$\epsilon = 1.0$	$\epsilon = 1.0$	$\epsilon = 4.0$
E_{elec}	-77.3	-13.4	-56.3	-14.1	-24.0	-6.0	-48.2	-12.1	-25.4	-20.2	-5.0
E_{vdW}	-56.5	-58.0	-57.4	-57.4	-58.2	-58.2	-59.8	-59.8	-60.1	-60.5	-60.5
E_{gas}	-133.8	-71.4	-113.7	-71.5	-82.3	-64.3	-108.2	-72.0	-85.5	-80.8	-65.7
E_{nonpolar}	-5.6	-5.8	-4.0	-4.0	-4.0	-4.0	-4.1	-4.1	-5.6	-3.9	-3.9
$E_{\text{PB/GB}}$	99.1	41.8	69.2	17.1	35.7	8.8	59.2	14.6	57.8	32.4	8.0
$E_{\text{solvation}}$	93.5	35.9	65.2	13.1	31.7	4.8	55.1	10.5	52.3	28.5	4.1
$E_{\text{PB/GB+elec}}$	21.8	28.4	12.9	3.0	11.8	2.8	11.0	2.6	32.5	12.2	3.0
$E_{\text{total,PB/GB}}$	-40.3	-35.4	-48.6	-58.5	-50.6	-59.5	-53.1	-61.5	-33.2	-52.4	-61.6

^a Force field. ^b Simulation time. ^c Orientation.

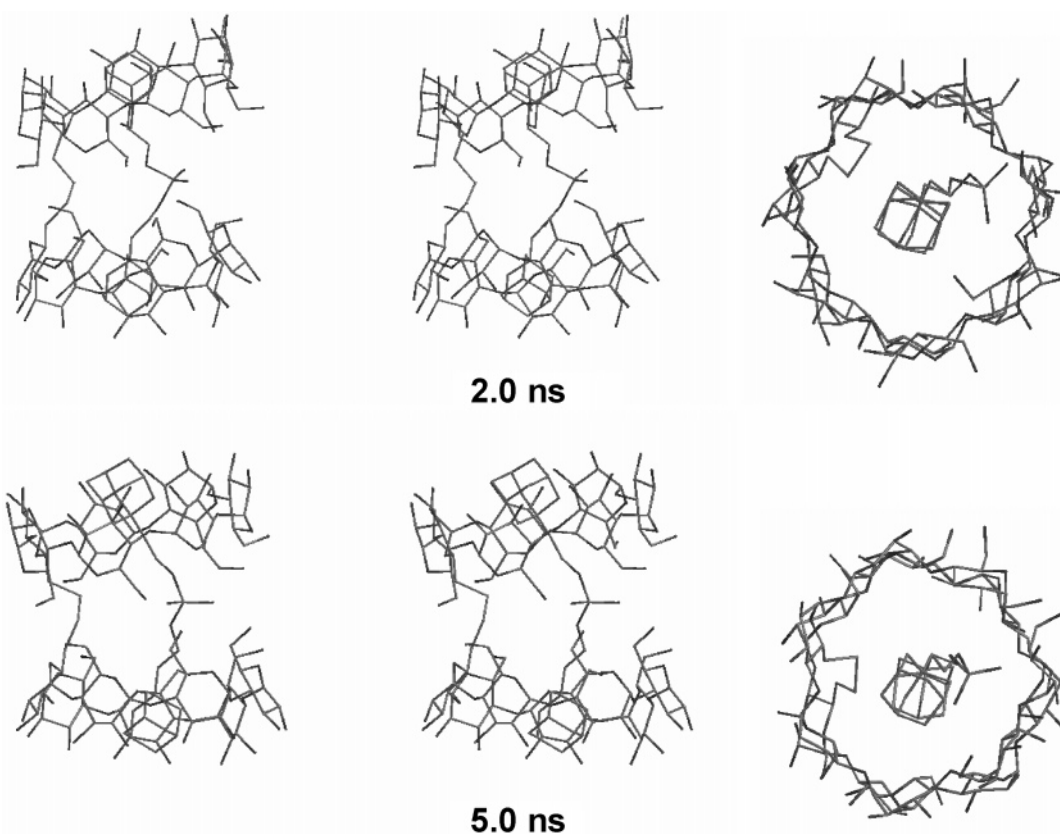


FIGURE 8. Representative conformations (a side view in stereo and a top view) obtained in the 5.0 MD simulations of the solvated ADA/BCDS complex. Hydrogen atoms were removed for clarity.

-22.3, -24.3, and -26.8 kcal/mol ($\epsilon = 1.0$) for the **H**, **T**, and **X** ADA 2:1 complexes were obtained from the 5.0 ns simulations, respectively. These estimates are of the same magnitude as for the complexation with the first **BCD** (Table 2, **C** (-26.3 kcal/mol)) and do not match the experimental observation that the enthalpy for the complexation of the second **BCD** is about half of the energy of binding of the first **BCD**.

Analysis of Entropy Contributions. Our efforts were further devoted to assess the entropy factors in these complexations. Unfavorable entropy contributions resulted in all cases (Table 4, Part I). The entropy favors the complexation with one **BCD** more than the complexation with two **BCDs**. Concerning the chelate effect, the entropy disfavors the complexation with two **BCDs** more than the complexation with the S-S linked dimer,

as expected from the classical interpretation of the chelate effect but in contradiction with the experimental results.⁶

A cautionary note has to be made here regarding the evaluation of the entropy contribution. It was computed exclusively for the molecules forming the complexes. The effect of the ordering or disordering of the water molecules around the complexes was not considered. Water molecules are intentionally removed whenever the MM/PBSA or MM/GBSA analyses are made. Consequently, this computational methodology reproduces the “classical” chelate effect but it is unlikely to be applicable in cases where changes in solvation apparently dominate the thermodynamics of the system.⁶ For now it is extremely difficult to evaluate by computation the entropy

TABLE 4. Computed Free Energies (ΔG , in kcal/mol) for the Complexation of ADA with One BCD, Two BCD and with the Dimer BCDS

	ADA												
	BCD						2BCD					BCDS	
	AMBER (parm94) ^a 500 ps ^b			AMBER (parm99) ^a 5.0 ns ^b			AMBER (parm94) ^a 500 ps ^b		AMBER (parm99) ^a 5.0 ns ^b			AMBER (parm94) ^a 500 ps ^b	AMBER (parm99) ^a 5.0 ns ^b
	down ^c	central ^c	up ^c	down ^c	central ^c	up ^c	H ^c	T ^c	H ^c	T ^c	X ^c		
I. MM/PBSA or MM/GBSA with ΔS Correction from AMBER(NMODE)													
<i>E</i> (total,PB/GB)													
$\epsilon = 1.0$	-19.8	-20.4	-18.7	-29.1	-26.3	-28.8	-40.3	-35.4	-48.6	-50.6	-53.1	-33.2	-52.4
$\epsilon = 4.0$				-36.6	-37.1	-35.2			-58.5	-59.5	-61.5		-61.6
<i>T</i> ΔS	-20.0	-16.7	-17.8	-19.1	-18.0	-17.5	-42.7	-37.0	-39.2	-35.3	-38.6	-21.2	-21.5
ΔG													
$\epsilon = 1.0$	0.2	-3.7	-0.9	-10.0	-8.3	-11.3	2.4	1.6	-9.4	-15.3	-14.5	-12.0	-30.9
$\epsilon = 4.0$				-17.5	-19.1	-17.7			-19.3	-24.2	-22.9		-40.1
II. Energy Minimized Structures with ZPE, ΔH_{vibr} , and ΔS_{vibr} Corrections from AMBER(NMODE)													
ΔH	-12.1	-1.9	-8.6	-20.1	-19.5	-15.9	-38.3	-17.7	-48.6	-39.1	-45.0	-24.0	-15.9
<i>T</i> ΔS	4.1	7.6	4.7	4.4	5.5	6.0	9.1	12.8	9.5	13.4	10.1	3.6	2.5
ΔG	-16.3	-9.5	-13.3	-24.5	-25.0	-21.9	-47.4	-30.5	-58.1	-52.5	-55.1	-27.6	-18.4
III. Energy minimized structures in solution (GBSA) with ZPE, ΔH_{vibr} and ΔS_{vibr} corrections from AMBER(NMODE)													
ΔH													
$\epsilon = 1.0$				-6.6	-0.8	-4.6			15.8	-5.0	9.2		-25.0
$\epsilon = 4.0$				-11.2	-9.4	-11.0			-19.1	-25.2	-25.5		-12.1
<i>T</i> ΔS				4.4	5.5	6.0			9.5	13.4	10.1		2.5
ΔG													
$\epsilon = 1.0$				-11.0	-6.3	-10.6			6.3	-18.4	-0.9		-27.5
$\epsilon = 4.0$				-15.6	-14.9	-17.0			-28.6	-38.6	-35.6		-14.6

^a Force field. ^b Simulation time. ^c Orientation.

changes for the whole system (complexed molecules and surrounding waters), and only a hypothesis can be formulated.

There should be diminished solvation in the dimer (**ADA/2BCD-H**) (recall that head orientation is proposed in this case and there are 28 hydroxyl groups unable to interact with water molecules) producing an entropy increase (higher disorder of the water arrangement). The corresponding difference between the complexed and the uncomplexed species for the chelate (**ADA/BCDS**) should not exist, and consequently its loss in solvation would likely be insignificant. It is seen from the comparison between the structures of the isolated **BCDS** molecule (Figure 3) and the complexed form **ADA/BCDS** (Figure 8) that the **BCDS** moiety is more compact. The isolated **BCDS** has some primary hydroxyl groups pointing toward the cavity and forming hydrogen bonds with other hydroxyl groups or even with the sulfur atoms. In contrast, most of these primary hydroxyl groups in the **ADA/BCDS** complex point toward the exterior and form hydrogen bonds with the water molecules. They should produce better solvation, thus lowering the entropy of the system. There are indications both from MD simulations and from PGSE NMR experiments that an increase of the rigidity of the macrocyclic structure strongly affects the surrounding water ordering,^{26–28} and as a consequence, the configurational entropy of the water molecules decreases. The overall effect is decrease of the entropy of the total system (solute plus water molecules). The complexes **ADA/BCD**, **ADA/2BCD**, and **ADA/BCDS** present an analogous situation with an expected decrease of entropy of water in the last case where the disulfide bridge significantly affects the freedom for motion when **BCDS** is complexed with **ADA**.

An alternative estimate of the free energies of the complexation was also made (Table 4, Part II). The energy minimized

structures with the lowest energies were only considered, selected among the extracted 6 or 51 structures from the 500 ps and the 5 ns MD trajectory files, respectively. The enthalpy differences were estimated by adding vibrational enthalpy corrections and zero-point energies. Vibrational contributions were only considered for ΔS . Indeed, in a qualitative agreement with experiment, the entropy of ditopic binding was determined in this case to be less favorable than for the monodentate binding. Moreover, in accord with experiment the entropy favors now the complexation with two BCDs more than the complexation with one BCD.

Part III of Table 4 presents results for the same approach but estimating the steric energy after minimization with accounting for the effect of the solvent (GBSA). The computed free energies for the complexation of **ADA/BCDS** are significantly less affected by the solvent than for **ADA/BCD** and **ADA/2BCD**. In qualitative agreement with the experimental data, the **ADA/BCDS** complex has less favorable free energies of complexation than **ADA/2BCD** when higher value is given ($\epsilon = 4.0$) of the dielectric parameter for estimating electrostatic interactions.

Conclusions

The results from the computational study (MM/PBSA and MM/GBSA) of the complexation between the adamantylphosphate and β -cyclodextrins revealed a clear preference for the binding with the **BCDS** in agreement with the experimental determinations.⁶ The guest has the central orientation (C) when complexed with one **BCD**.

We gained insight also into the relative importance of the enthalpy and the entropy contributions to the free energy of the complexation process. Experimental results⁶ (Table 1) indicate that the enthalpy favors the chelate effect by ca. 5 kcal/

(26) Naidoo, K. J.; Chen, J. Y.; Jansson, J. L. M.; Widmalm, G.; Maliniak, A. J. *Phys. Chem. B* **2004**, *108*, 4236–4238.

(27) Harano, Y.; Kinoshita, M. *Chem. Phys. Lett.* **2004**, *399*, 342–348.

(28) Choi, Y.; Jung, S. *Carbohydr. Res.* **2005**, *340*, 2550–2557.

mol, whereas entropy disfavors it by 8 kcal/mol. The computed binding enthalpy does favor the chelate effect (Table 4) when long enough simulations are executed. The entropy contribution originating from the host and the guest molecules always disfavors the complexation (Table 4, Part I). The binding with two **BCD** is disfavored, however, by about 35–40 kcal/mol, whereas that with the **BCDS** is disfavored only about 20 kcal/mol. An alternative estimate of the entropy differences (Table 4, Part II) is in a qualitative agreement with the experimental findings: the entropy favors more the formation of the complex with **2BCD** than with **BCDS**. Differences in the structural organization of the solvent around the complexed and the uncomplexed species must thus be crucial and very likely produce higher disorder for the complexation with two **BCD** units than in the complexation with the cyclodextrins dimerized with the S–S linker. Accordingly, the solvent effect on the computed free energies for the complexation of **ADA/2BCD** is higher than for **ADA/BCDS**. It was recently shown from studies on the influence of ligand, metal, and halogen nature on the chelate effect for complexes of group 14 element tetrahalides with monodentate and bidentate nitrogen-containing donors that

large reorganization energy shadows the chelate effect.²⁹ Thus, enthalpy contributions (from reorganization of the solvent molecules around the different species) that cannot be precisely estimated at present may have also influence on the final results.

Acknowledgment. Unfortunately, Professor P. A. Kollman is deceased; however, we would like to acknowledge his decisive contribution at the early stages of this research. The CESCO-C⁴ is gratefully acknowledged for allocating computational time. Financial support has been obtained from Ministerio de Ciencia y Tecnología, Spain (grant BQU2003-01231) and NSF, Bulgaria (project X-1406). CIRIT (Generalitat de Catalunya, Catalonia, Spain) and the “Ministerio de Educación, Cultura y Deporte” (Spain) are also acknowledged for a Visiting Professor grant to one of us (P.I.), and the UAB is thanked for a fellowship (I.B.).

Supporting Information Available: Snapshots of the complexes from different stages of the simulations. This material is available free of charge via the Internet at <http://pubs.acs.org>.

JO052469O

(29) Davidova, E. I.; Sevastianova, T. N.; Timoshkin, A. Y.; Suvorov, A. V.; Frenking, G. *Int. J. Quantum Chem.* **2004**, *100*, 419–425.